General Transfer Function for the Pinhole Camera

RICHARD E. SWING
Data Corporation (Eastern Division), 1254 Jefferson Davis Highway, Arlington, Virginia 22202
AND
DENNIS P. ROONEY
3370 Curtis Drive, Hillcrest Heights, Maryland 20023

(Received 15 September 1967)

The theory of partial coherence is applied to the classical pinhole camera. This study extends the previous work of Reynolds and Ward, and derives the general transfer function for the pinhole camera. System performance is covered for all field conditions, from Fresnel to Fraunhofer, in closed solution. From initial considerations of the one-dimensional case, a technique for generating low-frequency, controlled-modulation sinusoidal irradiance distributions is established; its transfer function is determined. Experimental evidence is introduced to support the theoretical contentions; agreement is obtained.

INDEX HEADINGS: Modulation transfer; Coherence; Resolving power.

ONE of the consequences of applying new analytical approaches to old physical problems is the additional insight often provided. These new approaches, typified in optics by the theory of partial coherence, permit a wider generality of application and often lead to a surprising analytical compactness of solution for many complex problems. This particular theory is concerned with relating optical observables (radiant flux measurements) and has demonstrated its theoretical and operational usefulness on a wide range of problems.

The pinhole camera is one of the classical problems of physical optics, and the description of its behavior constitutes probably the simplest nontrivial example of the successful application of scalar diffraction theory. However, until recently, the pinhole camera has not undergone the searching analysis provided by modern optical theory. While optimum pinhole size and impulse response (for the Fraunhofer case) can readily be calculated, little has been determined about its general transfer function, particularly for those camera geometries which are not Fraunhofer in nature. The standard specification of near-field impulse response in Fresnel integrals may have served to inhibit studies in this region.

In a recent paper,[1] Reynolds and Ward discussed the pinhole camera from the point of view of coherence theory. In that study, they concentrated on the resolution limit as a function of pinhole diameter and far-field distance, and were concerned primarily with impulse response. The purpose of this paper is to generalize the Reynolds and Ward results by deriving the complete transfer function for the pinhole camera system. The transfer function will be valid for all camera geometries within the paraxial approximation; interpretation of this transfer function will substantiate the explanation of the pertinent physics offered by Reynolds and Ward.

[1] G. Reynolds and J. Ward, J. Soc. Phot. Instr. Eng. 5, 3 (1966).

THE OPTICAL SYSTEM: GENERAL IMAGE IRRADIANCE (ONE DIMENSION)

We shall restrict the problem initially to one dimension, primarily to simplify the notation and establish the analytical approach with a minimum of mathematical encumbrances. A generalization to the two-dimensional case, for the pinhole camera, will then be made.

Consider the optical system of Fig. 1, where the pinhole (the slit in our one-dimensional analysis) will be located in the α plane. Both slit width and pinhole diameter will be denoted by 2ϵ. For descriptive convenience, the distances z_1 and z_2 will be termed object and image distances, respectively, although these designations may not be literally true for all geometries. The object plane will be illuminated with light whose coherence can be measured. Then the object can be completely described by the mutual-coherence function $\Gamma_0(\mu_1,\mu_2,\tau)$, or by the mutual intensity $\Gamma_0(\mu_1,\mu_2)$, when τ is made to vanish.

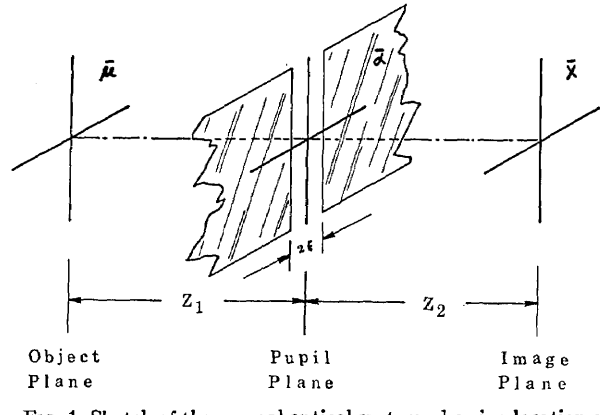

FIG. 1. Sketch of the general optical system, showing location of the pertinent planes, their corresponding coordinate systems, and the position and orientation of the slit. The aperture for the pinhole camera will also be located in this plane.

The amplitude transmittance of the slit, the aperture function, can be fully described by

$$\left.\begin{aligned} F(\alpha)&=1; \quad |\alpha|\leq\epsilon \\ &=0; \quad |\alpha|>\epsilon \end{aligned}\right\}. \tag{1}$$

Reference 1 outlines the general steps taken in relating the mutual intensity of object and image for this particular problem. The relationship stems from the application of the appropriate Green's functions to the solution of the Helmholtz equation which describes the optical propagation. It is therefore not necessary to repeat those steps, although a different analytical form is required; the physical rationale is the same for both. Then, for quasimonochromatic, partially coherent illumination and the standard paraxial approximations, the most general relation between object and image mutual intensity can be written[2]

$$\Gamma_i(x_1,x_2)=\int\int\int\int \Gamma_0(\mu_1,\mu_2)F(\alpha_1)F^*(\alpha_2)\cdot\left\{\exp\left[\frac{ik(\mu_1-\alpha_1)^2}{2z_1}\right]\exp\left[\frac{-ik(\mu_2-\alpha_2)^2}{2z_1}\right]\right.$$
$$\left.\cdot\exp\left[\frac{ik(\alpha_1-x_1)^2}{2z_2}\right]\exp\left[-\frac{ik(\alpha_2-x_2)^2}{2z_2}\right]\right\}\cdot d\mu_1 d\mu_2 d\alpha_1 d\alpha_2, \tag{2}$$

where

$$k=2\pi/\lambda, \tag{3}$$

and where * indicates the complex conjugate. The constant factors outside the integrals which arise from the description of the physics of propagation and those resulting from the paraxial approximations have been suppressed, since they will not be required for (nor their absence affect) the subsequent analysis.

When the exponentials in Eq. (2) are expanded, terms collected and the expressions regrouped, we obtain

$$\Gamma_i(x_1,x_2)=\exp\left[\frac{ik(x_1^2-x_2^2)}{2z_2}\right]\int\int\Gamma_0(\mu_1,\mu_2)\exp\left[\frac{ik(\mu_1^2-\mu_2^2)}{2z_1}\right]$$
$$\cdot\left\{\int F(\alpha_1)\exp\left[ik\left\{\frac{1}{2}\left(\frac{1}{z_1}+\frac{1}{z_2}\right)\alpha_1^2-\left(\frac{x_1}{z_2}+\frac{\mu_1}{z_1}\right)\alpha_1\right\}\right]d\alpha_1\right.$$
$$\left.\cdot\int F^*(\alpha_2)\exp\left[-ik\left\{\frac{1}{2}\left(\frac{1}{z_1}+\frac{1}{z_2}\right)\alpha_2^2-\left(\frac{x_2}{z_2}+\frac{\mu_2}{z_1}\right)\alpha_2\right\}\right]d\alpha_2\right\}d\mu_1 d\mu_2. \tag{4}$$

We will be interested in determining the observable, image irradiance. This is accomplished analytically by making the two image points coincident; i.e.,

$$I_i(x)=\Gamma_i(x_1,x_2)\big|_{x_1=x_2=x}. \tag{5}$$

Examination of Eq. (4) shows that the relation of Eq. (5) will eliminate the quadratic factor in x and remove the subscripts on the x's in the exponentials. We further will require incoherent illumination, since we will be concerned with transfer functions and these are defined without ambiguity only for such illumination.[3] This can be represented analytically for the present system by[4]

$$\Gamma_0(\mu_1,\mu_2)=I_0(\mu_1)\delta(\mu_1-\mu_2). \tag{6}$$

This is the usual representation for incoherent illumination, where the delta function implies that each point in the object is illuminated independent of all others, no matter how near. The paradoxical requirement of infinite energy does not enter nor affect the present consideration. Equation (6) is substituted in Eq. (4) in integral form,

$$\Gamma_0(\mu_1,\mu_2)=\int I_0(\mu)\delta(\mu_1-\mu)\delta(\mu-\mu_2)d\mu. \tag{7}$$

When Eqs. (5) and (7) are combined with Eq. (4), and the integrations carried out over μ_1 and μ_2, we obtain the irradiance in the x plane

$$I_i(x)=\int I_0(\mu)\cdot\left\{\int F(\alpha_1)\exp\left[ik\left\{\frac{1}{2}\left(\frac{1}{z_1}+\frac{1}{z_2}\right)\alpha_1^2\right.\right.\right.$$
$$\left.\left.\left.-\left(\frac{x}{z_2}+\frac{\mu}{z_1}\right)\alpha_1\right\}\right]d\alpha_1\int F^*(\alpha_2)\exp\left[-ik\left\{\frac{1}{2}\left(\frac{1}{z_1}+\frac{1}{z_2}\right)\alpha_2^2\right.\right.\right.$$
$$\left.\left.\left.-\left(\frac{x}{z_2}+\frac{\mu}{z_1}\right)\alpha_2\right\}\right]d\alpha_2\right\}d\mu. \tag{8}$$

Finally, since the integrals in α are complex and sym-

[2] All integrals in this paper, unless otherwise noted, are evaluated between $-\infty$ and ∞.

[3] R. Swing and J. Clay, J. Opt. Soc. Am. 57, 1180 (1967).

[4] M. Beran and G. Parrent, Jr., *Theory of Partial Coherence* (Prentice-Hall, Englewood Cliffs, N. J., 1964) p. 57.

metric, we can write

$$I_i(x)=\int I_0(\mu)\left|\int F(\alpha)\cdot\exp\left\{ik\left[\frac{1}{2}\left(\frac{1}{z_1}+\frac{1}{z_2}\right)\alpha_2-\left(\frac{x}{z_2}+\frac{\mu}{z_1}\right)\alpha\right]\right\}d\alpha\right|^2 d\mu. \quad (9)$$

This equation characterizes image formation for all system geometries, near and far fields, for incoherent illumination. The general system impulse response is given by the squared modulus of the inner integral.

Direct analytical development of this equation is not immediately feasible without the aid of simplifying assumptions, since the α integral is a general Fresnel integral having no closed solution in elementary functions. On the other hand, the α integral after quadrature is the system impulse response. Its Fourier transform is the system transfer function, the ultimate aim of this analysis. Before passing to consideration of this transfer function, however, it will be useful to simplify Eq. (9) for the Fraunhofer or far-field case. The far field occurs when the quadratic term in α becomes vanishingly small; i.e.,

$$[(2\epsilon)^2/\lambda][(1/z_1)+(1/z_2)]\ll 1, \quad (10)$$

since the actual limits on α are $\pm\epsilon$. This requires that

$$\begin{aligned} z_1&\gg(2\epsilon)^2/\lambda \\ z_2&\gg(2\epsilon)^2/\lambda. \end{aligned} \quad (11)$$

When these conditions are met, the quadratic term in the α integral becomes negligible, and Eq. (9) reduces to

$$I_i(x)=\int I_0(\mu)\,|\tilde{F}[(x/z_2)+(\mu/z_1)]|^2 d\mu, \quad (12)$$

where the tilde ($\sim$) denotes the Fourier transform of the aperture function. This is similar to Eq. (15) of Ref. 1, and represents the image as a convolution of the object irradiance with the impulse response of the slit. It constitutes the normal linear-system representation of the slit operating in the Fraunhofer mode.

Further deferring consideration of the general transfer function, we will find it useful to establish first a method for obtaining the transfer function for the more restricted, far-field case. Since it must necessarily be a limiting factor, this transfer function will aid in the development and interpretation of the more general case.

FAR-FIELD TRANSFER FUNCTION (ONE DIMENSION)

The far-field transfer function is given by the Fourier transform of the system impulse response. Thus,

$$\tilde{F}_{ff}(\sigma)=\int|\tilde{F}(x/z_2)|^2 e^{-2\pi i\sigma x}dx, \quad (13)$$

where we have used the Fourier shift theorem to remove the term in μ from the integral. The resultant exponential has been dropped, since it represents only a phase shift that occurs as a result of the displacement in $\bar{\mu}$. The integrand of Eq. (13) is now rewritten in terms of the integrals over the pupil plane,

$$\tilde{F}_{ff}(\sigma)=\int\left\{\int F(\alpha_1)\exp[-ikx\alpha_1/z_2]d\alpha_1 \cdot\int F^*(\alpha_2)\exp[ikx\alpha_2/z_2]d\alpha_2\right\}e^{-2\pi i\sigma x}dx. \quad (14)$$

These integrals are now rearranged to carry out the x integration first,

$$\tilde{F}_{ff}(\sigma)=\int\int F(\alpha_1)F^*(\alpha_2)\cdot\left\{\int\exp\left[-2\pi i\left(\sigma+\frac{\alpha_1}{\lambda z_2}-\frac{\alpha_2}{\lambda z_2}\right)x\right]dx\right\}d\alpha_1 d\alpha_2, \quad (15)$$

where the relation of Eq. (3) has been substituted for k in the exponentials. The inner integral becomes a delta function, and

$$\tilde{F}_{ff}(\sigma)=\int\int F(\alpha_1)F^*(\alpha_2)\delta\left(\sigma+\frac{\alpha_1}{\lambda z_2}-\frac{\alpha_2}{\lambda z_2}\right)d\alpha_1 d\alpha_2. \quad (16)$$

We now integrate over α_1 and obtain

$$\tilde{F}_{ff}(\sigma)=\int F(\alpha_2-\lambda z_2\sigma)F^*(\alpha_2)d\alpha_2. \quad (17)$$

This expression is the self-convolution of the aperture function with its complex conjugate, and is the classical definition of the transfer function. Since the aperture function is rectangular, Eq. (17) may be rewritten with the aid of Eq. (1) to give

$$\tilde{F}_{ff}(\sigma)=\frac{1}{2\epsilon}\int_{\lambda z_2\sigma-\epsilon}^{\epsilon}d\alpha_2, \quad (18)$$

which integrates easily, to become

$$\begin{aligned} \tilde{F}_{ff}(\sigma)&=1-(\lambda z_2/2\epsilon)\sigma; && |\sigma|\leq(2\epsilon/\lambda z_2) \\ &=0; && |\sigma|>(2\epsilon/\lambda z_2). \end{aligned} \quad (19)$$

This equation has long been known,[5] and shows the dependence of the transfer function on slit width, as well as the linear scaling with z_2. The necessary analytical approach has now been outlined, and we are finally prepared to consider the general case.

THE GENERAL SYSTEM TRANSFER FUNCTION

To derive the general transfer function, we return to the formulation of Eq. (8). The transfer function will be the Fourier transform of the impulse response, which, for the general case, is given by the two integrals over

[5] E. O'Neil, *Introduction to Statistical Optics* (Addison-Wesley Publishing Co., Inc., Reading, Mass., 1963), p. 79.

the pupil plane, $\bar{\alpha}$. We first define

$$a=\tfrac{1}{2}[(1/z_1)+(1/z_2)], \tag{20}$$

and then carry out the transformation, eliminating the μ term through the Fourier shift theorem, as before,

$$\tilde{F}(\sigma)=\int\left\{\int F(\alpha_1)\exp[ik(a\alpha_1^2-(x/z_2)\alpha_1)]d\alpha_1 \cdot\int F^*(\alpha_2)\exp[-ik(a\alpha_2^2-(x/z_2)\alpha_2)]d\alpha_2\right\}\cdot e^{-2\pi i\sigma x}dx. \tag{21}$$

Integration over x is next achieved, by first regrouping terms,

$$\tilde{F}(\sigma)=\int\int F(\alpha_1)F^*(\alpha_2)\exp[ika(\alpha_1^2-\alpha_2^2)]\cdot\left\{\int\exp[-2\pi i(\sigma+(\alpha_1/z_2)-(\alpha_2/z_2))x]dx\right\}\cdot d\alpha_1 d\alpha_2, \tag{22}$$

$$\tilde{F}(\sigma)=\int\int F(\alpha_1)F^*(\alpha_2)\exp[ika(\alpha_1^2-\alpha_2^2)]\cdot\delta\left(\sigma+\frac{\alpha_1}{\lambda z_2}-\frac{\alpha_2}{\lambda z_2}\right)d\alpha_1 d\alpha_2. \tag{23}$$

We then integrate over α_1, as before, and obtain

$$\tilde{F}(\sigma)=\exp[ika(\lambda z_2\sigma)^2]\int F(\alpha_2-\lambda z_2\sigma)F^*(\alpha_2)\cdot\exp[-ika(2\lambda z_2\sigma\alpha_2)]d\alpha_2. \tag{24}$$

The integration over α_2 can be accomplished by recalling the discussion preceding Eq. (18). Since the aperture functions are purely rectangular, and their convolution is only weighted by the exponential function in α_2, the same approach can be taken. We rewrite the integral of Eq. (24) in the light of Eq. (18) and obtain

$$\tilde{F}(\sigma)=\frac{1}{2\epsilon}\cdot\exp[ika(\lambda z_2\sigma)^2]\cdot\int_{\lambda z_2\sigma-\epsilon}^{\epsilon}\exp[-2\pi i(2az_2\sigma)\alpha_2]d\alpha_2. \tag{25}$$

This integral is easily evaluated. After application of limits, substitution of Eq. (20), and some subsequent manipulation, we obtain

$$\tilde{F}(\sigma)=\left[1-\frac{\lambda z_2\sigma}{2\epsilon}\right]\operatorname{sinc}\left[2\pi\epsilon\left(1+\frac{z_2}{z_1}\right)\sigma\left(1-\frac{\lambda z_2\sigma}{2\epsilon}\right)\right];\quad |\sigma|\leq 2\epsilon/\lambda z_2,$$
$$=0;\quad |\sigma|>(2\epsilon/\lambda z_2). \tag{26}$$

This is the general transfer function of the slit, irrespective of the field conditions, and valid for all possible geometries consistent with the paraxial approximation. The utility of first having determined the transfer function for the far-field case now becomes apparent. Not only is the far-field transfer function the limiting factor due to system geometry, but it also serves as the envellope of the oscillating sinc function. It is clearly the optimum transfer function for imaging purposes. The equation predicts system behavior to be similar to a lens out of focus. Indeed, it is nearly identical to the expression obtained by O'Neill[6] for an ideal cylindrical lens out of focus.

For near-field conditions, the function assumes negative values. This predicts spurious resolution, the manifestations of which are shown in Fig. 8 of Ref. 1. The experiments shortly to be described fully confirm this phenomenon and its characterization by Eq. (26).

EXPERIMENTS WITH THE ONE-DIMENSIONAL TRANSFER FUNCTION

It is relatively simple, in principle, to verify the transfer function of Eq. (26); we have done so with several types of experiments. The object consisted of a sinusoidal variable-area target of the kind described by Lamberts and Straub.[7] The illumination was provided by a light table with a heavy opal glass surface. The object was fastened directly to this surface; object illumination was then essentially incoherent, particularly since the object frequency α_0 never exceeded 0.20 cycles/mm. A Kodak Wratten number 58 filter was used to narrow the spectral width commensurate with the quasi-monochromatic approximation. The image plane contained a scanning photometer whose entrance slit was maintained parallel to the system slit.

Object modulation was known, and remained constant. The image modulation was determined from the trace produced by the scanning photometer. The value of the transfer function at the image frequency was then given by the ratio of the latter to the former modulation values, corrected for the photometer response.

Sine-Wave Generator

One of the interesting features of this system, which rendered the experiments more useful, is the variation of image spatial frequency with slit position. For a fixed object frequency, spatial frequency increases as the ratio of z_2/z_1 is decreased. Thus, the system becomes a sine-wave generator, and is ideally suited to produce low-frequency, controlled-modulation sinusoidal irradiance distributions; photographic-emulsion testing at very low spatial frequencies is an obvious application. Many others come to mind.

Under these circumstances, the system impulse re-

[6] See. Ref. 5, p. 94.
[7] R. Lamberts and C. Straub, J. Phot. Instr. Eng. 9, 331 (1965).

sponse, and hence the transfer function, is different for each value of z_2/z_1. It is therefore more useful to change Eq. (26) to accommodate this variation. Further, since it uses only one object frequency, corroborative tests are simplified; since the physics remain the same, verification of one will assure validity of the other.

First, we make the definitions

$$z_1+z_2=c, \tag{27}$$

$$\xi=z_1/z_2, \tag{28}$$

$$\sigma_i=\xi\sigma_0. \tag{29}$$

The first requires that the distance between the object and image planes remains constant for a set of determinations in which ξ is made to vary. The second establishes the origin at $z_1=0$, and orders the independent variable conventionally, from left to right. Equation (29) shows the relation between image and object frequency produced by the change of slit position.

When Eqs. (27)–(29) are applied to Eq. (26), we obtain

$$\tilde{F}(\xi)_{\sigma_0}=\left[1-\frac{\lambda\sigma_0 c\xi}{2\epsilon(1+\xi)}\right]\cdot\operatorname{sinc}\left[2\pi\epsilon\sigma_0(1+\xi)\left\{1-\frac{\lambda\sigma_0 c\xi}{2\epsilon(1+\xi)}\right\}\right], \tag{30}$$

the transfer function of the sine-wave generator.

Experimental Results

Figure 2 shows plots of Eq. (30) for selected values of the parameters, with c constant at 100 cm. Experimental points are added to the figure and indicate a generally excellent agreement with the predicted values. Spurious resolution was observed for the 1-mm-slit response; the observed pattern clearly shifted phase in the image plane.

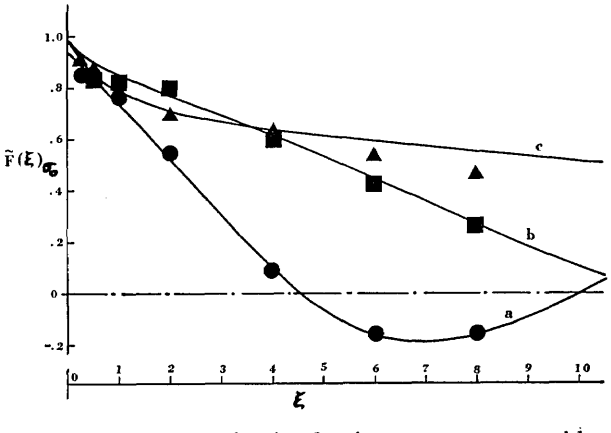

FIG. 2. Transfer function for the sine-wave generator, with a constant object frequency, σ_0, of 0.20 cycles/mm and a total object-to-image distance of 100 cm. Curve (a) (●): $2\epsilon=1$ mm; Curve (b) (■): $2\epsilon=\frac{1}{2}$ mm; Curve (c) (▲): $2\epsilon=\frac{1}{4}$ mm. Points shown are experimental; curves are calculated from Eq. (30).

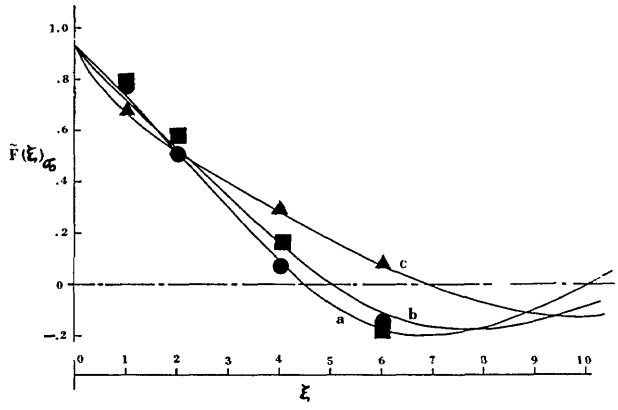

FIG. 3. Transfer function for the sine-wave generator, with a constant object frequency, σ_0, of 0.20 cycles/mm and a slit width of 1 mm. The points shown are experimental; curves are calculated from Eq. (30). Curve (a) (●): $c=1$ m; Curve (b) (■): $c=2$ m; Curve (c) (▲): $c=4$ m.

For the far-field portion of the general transfer function, a reciprocal relation exists between c and 2ϵ. Thus, response should remain the same when one is doubled, the other halved. However, this reciprocity does not exist in the argument of the sinc function, and we should, therefore, expect a qualitative change for the same slit width when the system length is increased. Figure 3 shows this variation, with the slit width held constant at 1 mm. Some experimental points are shown; the number of them is limited by the experimental difficulty of achieving sufficient irradiance in the image plane for the longer distances. Agreement is again excellent.

PINHOLE-CAMERA TRANSFER FUNCTION

We have sufficiently established the validity of the one-dimensional case to proceed to the pinhole, or two-dimensional case. Fortunately, it will not be necessary to repeat the steps leading to Eq. (26), with the obvious complexity demanded by the added dimension. We can derive the appropriate transfer function entirely by analogy.

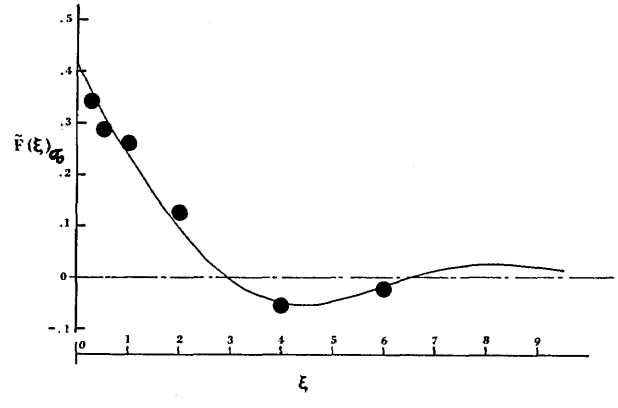

FIG. 4. Transfer function for a pinhole camera operating in a typically near-field mode. The object frequency, σ_0, is 0.375 cycles/mm, with the pinhole diam (2ϵ) 1 mm and a total object-to-image distance of 100 cm. Points shown are experimental; the curve is calculated from Eq. (34).

The two-dimensional version of the transfer function for the far-field condition is simply the self-convolution of a clear, circular aperture with its complex conjugate, the analytical details of which are adequately described by O'Neill.[8] After adjusting constants and variables to fit the present problem, we obtain for a pinhole of diameter 2ϵ

$$\tilde{F}_{ff}(\sigma)=\frac{2}{\pi}\left\{\cos^{-1}\left[\frac{\lambda z_2\sigma}{2\epsilon}\right]-\left[\frac{\lambda z_2\sigma}{2\epsilon}\right]\left[1-\left(\frac{\lambda z_2\sigma}{2\epsilon}\right)^2\right]^{\frac{1}{2}}\right\}. \quad (31)$$

This expression describes the transfer characteristics of the pinhole camera operating in a condition analogous to infinite conjugates for a lens.

The two-dimensional, circular equivalent to the sinc-function is the Bessel function of the first kind divided by its argument

$$\text{Bessinc}(\beta)=J_1(\beta)/\beta. \quad (32)$$

By analogy, then, we can specify the entire transfer function; this will describe the pinhole-camera performance at all conjugate distances. Thus,

$$\tilde{F}(\sigma)=\tilde{F}_{ff}(\sigma)\ \text{Bessinc}\{2\pi\epsilon[1+(z_2/z_1)]\sigma\tilde{F}_{ff}(\sigma)\}. \quad (33)$$

For experimental tests, it will be more convenient to change spatial frequency by moving the pinhole longitudinally. We therefore require a circular, two-dimensional analog to Eq. (30). When the definitions of Eqs. (27)–(29) are coupled with Eqs. (32) and (33), the sine-wave-generator transfer function becomes

$$\tilde{F}(\xi)_{\sigma_0}=\tilde{F}_{ff}(\xi)_{\sigma_0}\ \text{Bessinc}\{2\pi\epsilon\sigma_0(1+\xi)\tilde{F}_{ff}(\xi)_{\sigma_0}\}, \quad (34)$$

where

$$\tilde{F}_{ff}(\xi)_{\sigma_0}=\frac{2}{\pi}\left\{\cos^{-1}\left[\frac{\lambda\sigma_0 c\xi}{2\epsilon(1+\xi)}\right]-\left[\frac{\lambda\sigma_0 c\xi}{2\epsilon(1+\xi)}\right]\left[1-\left(\frac{\lambda\sigma_0 c\xi}{2\epsilon(1+\xi)}\right)^2\right]^{\frac{1}{2}}\right\}. \quad (35)$$

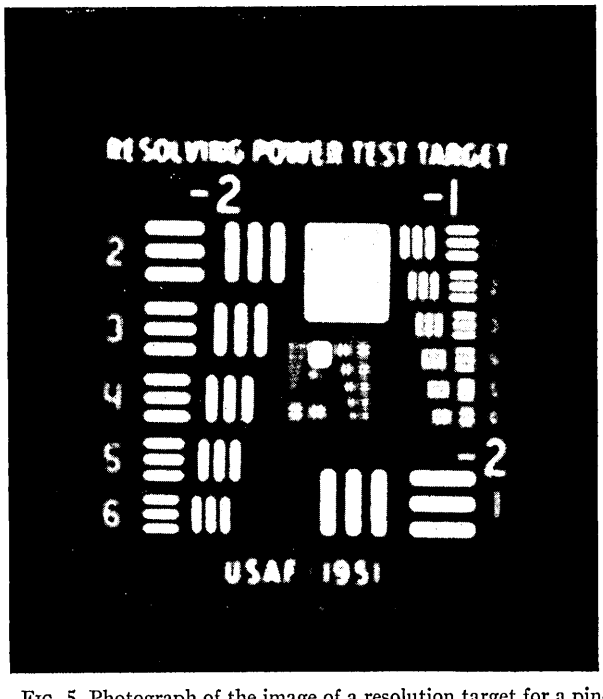

FIG. 5. Photograph of the image of a resolution target for a pinhole system operating in the near-field mode. Here, $c=1$ m, $(2\epsilon)=1$ mm, and $\xi=1.0$. Spurious resolution can be seen for targets after pattern group $(-1, 5)$.

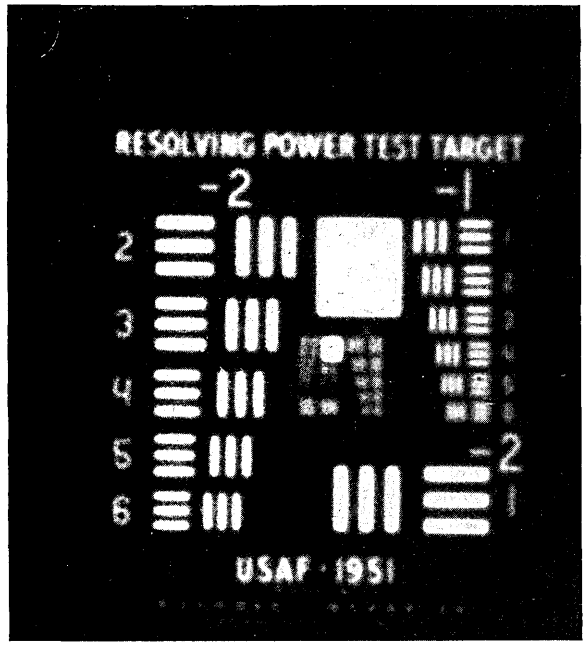

FIG. 6. Photograph of the image of a resolution target for a pinhole-camera system operating in the far-field mode. For this system, $c=4$ m, $(2\epsilon)=1$ mm, and $\xi=1.0$. Experimentally observed resolution limit is the $(-1, 5)$ pattern group, or 0.80 cycles/mm; the calculated value is 0.77 cycles/mm.

Experimental Results

Figure 4 shows a plot of this function for a pinhole diam (2ϵ) of 1 mm and a system length (c) of 100 cm. Experimental points are added to the figure and indicate good agreement. The simple variable-area sinusoidal targets employed in the slit experiments were not used for these tests. Instead, targets whose optical transmittance varied sinusoidally in one dimension[9] were used. The procedure for obtaining values of the transfer function was essentially the same as that used for the slit determinations. However, since these targets are photographic they tend to scatter, and modulation transfer values are therefore not as inherently accurate as those shown in Figs. 2 and 3. General agreement with the predicted values is nevertheless good.

The curve of Fig. 4 predicts spurious resolution. To exhibit this, resolution targets were photographed under

[8] See. Ref. 5, p. 84.

[9] N. Kapany, J. Eyer, and R. Shannon, J. Opt. Soc. Am. 47, 103 (1957).

the physical-system conditions appropriate to the curve. One of these is shown in Fig. 5. The three-bar pattern can be observed out to group $(-1, 5)$. Here it vanishes, as the contrast drops to zero. Subsequent groups show a clear phase reversal, evidenced by the two-bar pattern. The theoretical cross-over spatial frequency calculated from Eq. (34) is slightly greater than 0.80 cycles/mm, which lies between pattern groups $(-1, 5)$ and $(-1,6)$. Again, the agreement between theory and experiment is excellent.

When far-field conditions on the slit are met, there should be a gradual decrease of resolution, without spurious resolution, as predicted by Eq. (31). The far-field distance for the 1-mm-diam pinhole with a mean wavelength of 530 mμ is approximately 1.9 m. The system response when $z_1 > 1.9$ m and $z_2 > 1.9$ m should be approximately far field. This is demonstrated in the photograph in Fig. 6, where $c = 4$ m and the pinhole diameter is 1 mm. The object resolution limit, calculated according to the classical Rayleigh criterion[10] should be approximately 0.80 cycles/mm for the experimental conditions. Since object and image distances were identical and equal to 2 m, the object and image frequencies were also identical. The resolution observable in the figure is pattern group $(-1,5)$, or 0.80 cycles/mm, substantiating the hypothesis of the far-field response. The gradual loss of contrast with increasing target frequency is clearly shown and further indicates the expected response. No spurious resolution can be observed.

[10] See Ref. 1, Eq. (23).

CONCLUDING REMARKS

The concepts of the theory of partial coherence applied to the classical pinhole camera system have led to the derivation of the general transfer function governing its behavior with incoherent illumination. The experimental evidence is in excellent agreement with the theoretical predictions. Response for any paraxial system is fully described, whether in the Fresnel or Fraunhofer regions. Incident to this, a technique for generation of low-frequency, controlled-modulation sinusoidal irradiance distributions has been described, and its transfer function determined. The results of this investigation, both analytical and experimental, have proceeded from and complement the studies of Reynolds and Ward. The analytical characterization and understanding of the physics of the pinhole camera is thus modernized once more.

ACKNOWLEDGMENT

The authors wish to thank Paul Glascock for his valuable assistance with some phases of the experimental work.

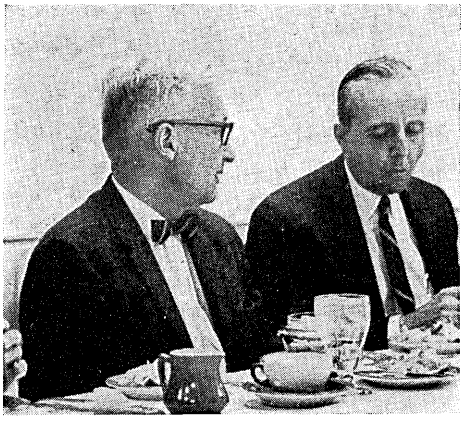

Francis Turner (*president-elect*) and William Koch (*Director*, AIP) at meeting of Board of Directors in Detroit, 10 October.

Bruce Billings (r.) and Walter Driscoll (editor of *Handbook of Optics*) at meeting of Board of Directors in Detroit, 10 October.